

# The two-pore channel TPCN2 mediates NAADP-dependent $\text{Ca}^{2+}$ -release from lysosomal stores

Xiangang Zong · Michael Schieder · Hartmut Cuny · Stefanie Fenske ·  
Christian Gruner · Katrin Rötzer · Oliver Griesbeck · Hartmann Harz ·  
Martin Biel · Christian Wahl-Schott

Received: 30 May 2009 / Accepted: 2 June 2009 / Published online: 26 June 2009  
© The Author(s) 2009. This article is published with open access at Springerlink.com

**Abstract** Second messenger-induced  $\text{Ca}^{2+}$ -release from intracellular stores plays a key role in a multitude of physiological processes. In addition to 1,4,5-inositol trisphosphate ( $\text{IP}_3$ ),  $\text{Ca}^{2+}$ , and cyclic ADP ribose (cADPR) that trigger  $\text{Ca}^{2+}$ -release from the endoplasmic reticulum (ER), nicotinic acid adenine dinucleotide phosphate (NAADP) has been identified as a cellular metabolite that mediates  $\text{Ca}^{2+}$ -release from lysosomal stores. While NAADP-induced  $\text{Ca}^{2+}$ -release has been found in many tissues and cell types, the molecular identity of the channel (s) conferring this release remained elusive so far. Here, we

show that TPCN2, a novel member of the two-pore cation channel family, displays the basic properties of native NAADP-dependent  $\text{Ca}^{2+}$ -release channels. TPCN2 transcripts are widely expressed in the body and encode a lysosomal protein forming homomers. TPCN2 mediates intracellular  $\text{Ca}^{2+}$ -release after activation with low-nanomolar concentrations of NAADP while it is desensitized by micromolar concentrations of this second messenger and is insensitive to the NAADP analog nicotinamide adenine dinucleotide phosphate (NADP). Furthermore, TPCN2-mediated  $\text{Ca}^{2+}$ -release is almost completely abolished when the capacity of lysosomes for storing  $\text{Ca}^{2+}$  is pharmacologically blocked. By contrast, TPCN2-specific  $\text{Ca}^{2+}$ -release is unaffected by emptying ER-based  $\text{Ca}^{2+}$  stores. In conclusion, these findings indicate that TPCN2 is a major component of the long-sought lysosomal NAADP-dependent  $\text{Ca}^{2+}$ -release channel.

Xiangang Zong and Michael Schieder contributed equally to this work.

**Electronic supplementary material** The online version of this article (doi:10.1007/s00424-009-0690-y) contains supplementary material, which is available to authorized users.

X. Zong · M. Schieder · H. Cuny · S. Fenske · C. Gruner ·  
K. Rötzer · M. Biel · C. Wahl-Schott  
Center for Integrated Protein Science CIPS-M and Zentrum  
für Pharmaforschung, Department Pharmazie,  
Ludwig-Maximilians-Universität München,  
Butenandtstr. 5-13,  
81377 Munich, Germany

O. Griesbeck  
Max Planck Institute of Neurobiology,  
Martinsried, Germany

H. Harz  
BioImaging Zentrum der Ludwig-Maximilians-Universität München,  
Munich, Germany

M. Biel (✉) · C. Wahl-Schott (✉)  
Department Pharmazie, Pharmakologie für Naturwissenschaften,  
Ludwig-Maximilians-Universität München,  
Butenandtstr. 5-13,  
81377 München, Germany  
e-mail: martin.biel@cup.uni-muenchen.de  
e-mail: christian.wahl@cup.uni-muenchen.de

**Keywords** TPCN2 · Two-pore channels · NAADP ·  
 $\text{Ca}^{2+}$ -release · Lysosome · Acidic stores

## Introduction

$\text{Ca}^{2+}$ -release from intracellular stores is a fundamental cellular process that is involved in the control of numerous physiological functions including muscle contraction, secretion, cell motility, and control of immune response [3, 11]. Given the diversity and complexity of these processes, it does not come as a surprise that  $\text{Ca}^{2+}$ -release is controlled by a complex array of signaling pathways and second messengers [19, 23, 29, 32]. NAADP is the latest entry in the list of  $\text{Ca}^{2+}$ -releasing molecules [19, 20]. This molecule is synthesized in the cell by ADP cyclases by exchanging the nicotinamide moiety of NADP with

nicotinic acid [21]. Notably, among all known  $\text{Ca}^{2+}$ -releasing agents, NAADP is the most potent one acting in the low-nanomolar concentration range [14]. The  $\text{Ca}^{2+}$ -releasing activity of NAADP was first discovered in the mid-1990s in acidic lysosome-related organelles of sea urchin eggs [20] and has since been demonstrated in many mammalian tissues and cell types [13, 17]. NAADP-mediated  $\text{Ca}^{2+}$ -release is characterized by a number of characteristic features. First of all, NAADP-dependent  $\text{Ca}^{2+}$ -release displays a characteristic bell-shaped dose-response curve with a peak in the low nanomolar concentration range and total loss of activity at high micromolar concentrations [8, 22]. Moreover, the native NAADP-dependent  $\text{Ca}^{2+}$ -release channel is insensitive to NADP which differs from NAADP only by the replacement of a carboxyl by an amid group [15]. Finally, in contrast to  $\text{IP}_3$ - and  $\text{Ca}^{2+}$ /cADPR-sensitive stores, NAADP mainly seems to induce  $\text{Ca}^{2+}$ -release from acidic lysosomal stores [10, 13], although in some cell types, NAADP-mediated  $\text{Ca}^{2+}$ -release was also found in ER-derived stores, including the nuclear envelope [15].

The molecular identity of the cellular NAADP receptor has been a matter of controversy [13, 17]. It was suggested that there may be no unique receptor for NAADP but that NAADP, like  $\text{Ca}^{2+}$  and cADPR, is an agonist of the ryanodine receptor (RyR) complex present in ER-derived calcium stores [15]. Other studies suggested that members of the transient receptor potential (TRP) channel family including TRPM2 [1] and TRPM1 [34] may be the cellular target protein of NAADP. However, the micromolar concentrations of NAADP required to fully activate these channel are one to two orders higher than those found for NAADP-mediated  $\text{Ca}^{2+}$ -release in a variety of cells. Since none of the so-far analyzed proteins matches the hallmarks of native NAADP-sensitive release channels in a satisfying fashion, we hypothesized that the major receptor of NAADP may be formed by another not yet characterized protein.

## Materials and methods

### Cloning of TPCN1 and TPCN2

For cloning of TPCN1, two cDNA fragments were amplified from mouse brain RNA by RT-PCR using the SuperScript III-One-Step Kit (Invitrogen; primers for fragment 1: TTA GAA ATG CCT CTG ATG GAA and ATG CTT TGA GGT GAA ATT CCC A; primers for fragment 2: CAG ACA GCA TTG GTT TGA TGA G and GTG GGG TTT CTT CCT AGT GGT CTC GAG CCT CAT ACC AGA CAC AGA CAC). Following restriction digests, the two fragments were assembled in pcDNA3 using the Hind III site in the 5' untranslated region, the

central EcoR I site, and the Xho I site generated by PCR in the 3' untranslated region (fragment 1=1,413 bp, fragment 2=1,548 bp). For cloning of TPCN2, the complete open-reading frame was amplified from mouse brain RNA. The forward primer (GGC TGT GGT ACC GCC ACC ATG GCG GCA GAA GAG CAG C) binds to the 5' end and contains a Kozak consensus sequence and a Kpn I restriction site for cloning; the reverse Primer (GCC GCT CGA GAG GCC AGC ATC TCT GTC CTG) binds to the 3' untranslated region and contains a Xho I restriction site for cloning. After restriction digest with KpnI and XhoI, the 2,255-bp fragment was cloned into pcDNA3 vector (Invitrogen). All cloned sequences were verified by sequencing.

### Northern blot

A mouse multiple tissue Northern blot (Applied Biosystems/Ambion, Austin, TX) containing 2  $\mu\text{g}$  poly(A) RNA from heart, brain, liver, spleen, kidney, lung, thymus, testis, ovary, and embryo was hybridized with probes against TPCN1 and TPCN2. Probes covered the entire coding regions and were generated by random-primed labeling with a  $\alpha^{32}\text{P}$ -dCTP (Roche, Basel, Switzerland). The membrane was hybridized overnight in stringent conditions. After two washing steps, the hybridized probe was visualized with a phosphorimager after an exposure time of 24 h or using a film (Hyperfilm MP, GE Healthcare, Piscataway, NJ) after a radiographic exposure time of 14 days at  $-80^\circ\text{C}$ . The same blot was probed subsequently with TPCN1 and TPCN2 probes. The blot was stripped between each hybridization with SDS-containing buffer.

### Production of TPCN2-specific antibodies

Polyclonal rabbit antisera were raised against a peptide (CDILE EPKEE ELMEK LHKHP) corresponding to aa 707 to 725 of TPCN2 plus a N-terminal cysteine. For affinity purification of antibodies, the peptide was coupled to SulfoLink Coupling Gel (Thermo Fisher Scientific, Waltham, USA) in a column. Serum was loaded onto column and washed. Bound antibodies were eluted with 100 mM Glycin-HCl pH 2.8 in 800  $\mu\text{l}$  aliquots and immediately neutralized with Tris-base.

### Deglycosylation assay

The glycosylation deficient TPCN2 mutant (N594Q/N601Q) was cloned using the QuickChange Kit (Stratagene, La Jolla, CA). The deglycosylation assay was performed as described previously [25]. Briefly, HEK293 cells were transfected with TPCN2, TPCN2N594Q/N601Q, or EGFP-TPCN1 using the calcium phosphate method and lysed; 10  $\mu\text{g}$  of

whole-cell lysates were incubated in the presence or absence of PNGase F or endoglycosidase H (both New England Biolabs, Ipswich, MA), according to the manufacturer's instruction. The protein denaturation was performed for 10 min at 45°C, the enzyme incubation for 1 h at 37°C. Cell lysates were then analyzed. Subsequently, proteins were subjected to Western blot analysis.

#### Coimmunoprecipitation in HEK293 cells

For coimmunoprecipitation experiments, TPCN2 and TPCN1 fusion proteins were generated with either myc tag fused at the N-terminus or with EGFP sequence fused at the N-terminus. For expression of recombinant proteins, HEK293 cells were transfected using the calcium phosphate method. Three days after transfection, HEK293 cells were lysed as described previously [30]. Equal amounts of protein (measured by Bradford assay) were incubated overnight at 4°C with 40 µl of protein A-Sepharose (GE Healthcare, Chalfont St. Giles, UK) and a specific antibody (Cell Signaling Technology, Beverly, MA) directed against the myc tag of examined proteins and 500 µl of buffer containing 50 mM Tris HCl (pH 7.4), 150 mM NaCl, 1 mM EDTA, and 50 mM Triton X-100, supplemented with PI. Beads were pelleted by centrifugation and washed three times with cold buffer containing 20 mM Tris HCl (pH 7.4), 5 mM MgCl<sub>2</sub>, 0.5 mM DTT, 20% (v/v) Glycerol supplemented with PI. Interacting proteins were visualized after boiling for 5 min in Laemmli sample buffer by SDS/PAGE, Western blot analysis, and ECL (GE Healthcare). The antibodies used were as follows: anti-GFP for detection of EGFP-TPCN2 fusion protein. An antibody against GST (GE Healthcare) was used as control.

#### Immunocytochemistry

For immunodetection, COS-7 cells grown on glass coverslips in a 24-well plate were transiently transfected with TPCN2 cDNA using Fugene 6 (Roche Diagnostics). Cells were cultured in DMEM supplemented with 10% fetal calf serum and kept at 37°C, 10% CO<sub>2</sub> and fixed 1 or 2 days after transfection with 4% paraformaldehyde in PBS. Cells were permeabilized and blocked with 0.5% Triton X-100 and 5% Chemiblock (Millipore, Billerica, USA) in PBS. Cells were incubated with anti-TPCN2 (1:1000), anti-Myc (Cell Signaling, Danvers, MA; 1:1,000), anti-GFP (Clontech, Mountain View, USA; 1:500), anti-HA (Cell Signaling; 1:1000), anti-lamp1 (Abcam, Cambridge, USA; 1:250), and anti-Calnexin (Santa Cruz Biotechnology, Santa Cruz, USA; 1:100) primary antibodies in 2% Chemiblock (Millipore) and 0.3% Triton X-100 for 1 h. Then, cells were washed four times with PBS for 5 min each and incubated with AMCA (1:100), Cy2 (1:200), Cy3 (1:400), and Cy5 (1:400)

secondary antibodies (all Jackson ImmunoResearch, West Grove, PA) in 2% Chemiblock (Millipore) for 1 h. Unbound antibodies were removed by three washing steps with PBS. For the staining of membranes and organelles, TRITC-WGA (membranes; 1:100; Sigma), Mitotracker Red CMX Ros (Mitochondria; 1:1,500; Invitrogen), and Hoechst 33342 (Nuclei; 0.4 µg/ml; Invitrogen) were used according to manufacturers' instructions. For visualization of lysosomes, in some experiments, a lamp1-EGFP fusion protein was co-expressed with TPCN2 (kind gift of Esteban C. Dell'Angelica, Dept Human Genetics, UCLA, USA). The glass coverslips were then mounted onto glass slides with Permafluor (Sigma, St. Louis, MO). Cells were visualized under a Zeiss LSM 510 laser confocal microscope as previously described [25].

#### Cell surface expression

To determine surface expression of TPCN2 in COS-7 cells, the HA epitope was inserted into the loop between the putative first and second transmembrane domains of TPCN2. Two mutagenic primers (GTC GGG AAC ATC GTA TGG GTA AGT CTT TGT GAA GGA AGA TGG G and TAC GAT GTT CCC GAC TAC GCA GAT GTG CGC TAC CGT TC) have been used to insert the hemagglutinin sequence (YPYDVPDYA) in frame between amino acid residues 92 and 93 of TPCN2 using the QuikChange Kit (Stratagene) according to the manufacturer's instruction. The sequence has been verified by sequencing. After transfection, cells were analyzed by immunocytochemistry as described above except for omitting the permeabilization step with Triton X-100 (nonpermeabilized cells). Control cells were treated equally but permeabilized.

#### Ca<sup>2+</sup> imaging

Two days after transfection with TPCN2-EGFP or with the empty EGFP vector using Fugene 6 (Roche, Basel, Switzerland), HEK293 cells were loaded with Fura-2AM (5 µM) before measuring [Ca<sup>2+</sup>]<sub>i</sub> and subsequently placed in extracellular recording solution containing (in mM) 140 NaCl, 5 KCl, 3 MgCl<sub>2</sub>, 10 glucose, and 10 HEPES, pH 7.4. The fluorescence intensity of individual patch-clamped cells was monitored with a dual excitation fluorometric system using a Carl Zeiss Axiovert 135 fluorescence microscope equipped with a ×40 Plan-Apochromat 1.3 oil objective. The monochromatic light source (Polychrom II, TILL-Photonics) was tuned to excite Fura-2 fluorescence at 340 nm (F340) and 380 nm (F380) with a sampling frequency of 0.5 Hz for 3 ms each. Emission was detected at 450–550 nm using a PCO SensiCam VGA camera (Kelheim, Germany) and recorded and analyzed using

**Fig. 1** Properties of two-pore channels. **a** *Upper panel* Transmembrane topology of TPCN1 and TPCN2. The predicted N-glycosylation sites are marked by red forks. *Lower panel* Schematic representation of the primary sequence of TPCN1 and TPCN2. The degree of sequence identity within the N- and C-termini, the two transmembrane building blocks and the interdomain linker is indicated. **b** Mouse multiple tissue northern blots of TPCN1 (*left panel*) and TPCN2 (*right panel*) demonstrate expression in all tissues investigated. **c** EGFP-TPCN1 (*upper panel*) and EGFP-TPCN2 (*lower panel*) channels expressed in HEK293 cells are localized intracellularly (*green* TPCN channels; *red* membrane marker, *blue* nuclei; *scale bar* 5  $\mu$ m). **d** Western blots with lysates from HEK293 cells containing myc-tagged TPCN1 (*left panel*), wild-type TPCN2 (*middle panel*), and a glycosylation-deficient TPCN2 double-mutant (TPCN2-Q; *right panel*). Ten micrograms of protein were applied per lane. **e** Lysates of HEK293 cells cotransfected with myc-tagged TPCN2 and EGFP-tagged TPCN2 (*lanes 1–3*) or myc-tagged TPCN1 and EGFP-tagged TPCN2 (*lanes 6–8*) were immunoprecipitated with anti-myc antibody (*lanes 2, 5, 7*) or anti-GST (control, *lanes 3 and 8*), blotted and probed with anti-GFP. *Lanes 1, 6* input, *lane 4* negative control

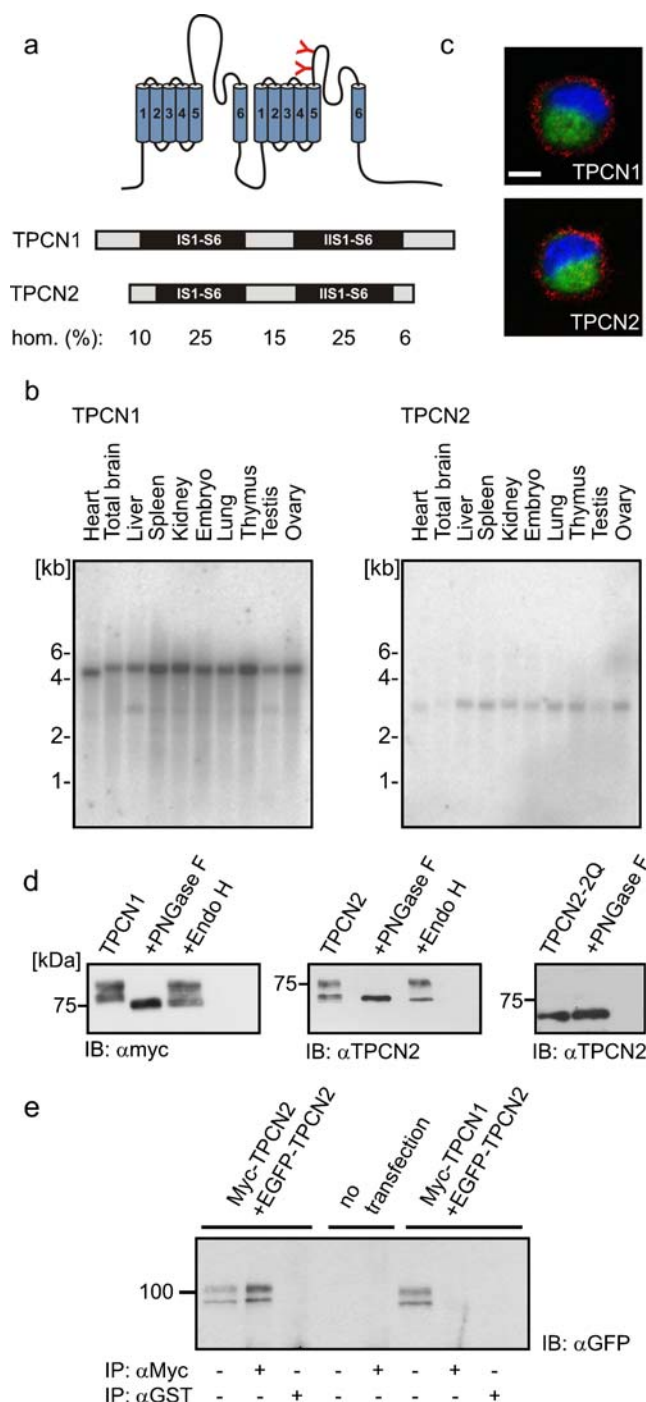
Tillvision (Till Photonics, Martinsried, Germany). For internal perfusion with NAADP, NADP, or IP<sub>3</sub>, Fura-2AM-loaded HEK293 cells were patched in standard whole-cell configuration. After establishing base line  $[Ca^{2+}]_i$ , the membrane was perforated, and the recording was continued in current clamp mode ( $I=0$ ) [4]. Patch pipette solution contained in mM—140 KCl, 10 HEPES, 1 MgCl<sub>2</sub>, and 0.05 BAPTA (pH 7.4) [6]. Fura-2 (pentapotassium salt, Invitrogen, Carlsbad, USA) was added to the standard internal solution at 7  $\mu$ M in addition to preloading. Changes in Fura-2 fluorescence are reported as the fluorescence ratios ( $F_{340}/F_{380}$ ) and are translated into apparent intracellular calcium concentration according to [16].

## Statistics

All values are given as mean $\pm$ SEM;  $n$  is the number of experiments. An unpaired  $t$  test was performed for the comparison between two groups. Significance was tested by ANOVA followed by Dunnett test if multiple comparisons were made. Values of  $P<0.05$  were considered significant.

## Results

In our search for novel intracellular  $Ca^{2+}$ -release channels, we analyzed mammalian homologs of the two-pore cation channel TPC1, a  $Ca^{2+}$ -activated release channel identified in the vacuolar membrane of *Arabidopsis thaliana* and other plants [26]. A rat homolog of TPC1, designated TPCN1 was originally cloned from rat kidney but was not functionally characterized [18]. Based on sequence data from the gene bank, we cloned full-length murine TPCN1 and a novel homolog of this channel, TPCN2. Murine TPCN1 and TPCN2 show an overall sequence identity of



about 20% to each other and to plant TPC1 [26] (Fig. 1a, Supplementary Fig. S1). TPCN channels represent a distinct branch within the superfamily of pore-loop channels [12, 31]. They are composed of two homologous building blocks each containing six transmembrane helices (S1–S6) and an ion-conducting pore loop between S5 and S6. The two putative pore loops of TPCN1 and TPCN2 show substantial homology to the pore of TPC1. In contrast to TPC1 both murine channels do not contain EF hand



motifs that may act as  $\text{Ca}^{2+}$  sensors in TPC1. Transcripts of TPCN1 and TPCN2 are widely expressed in the body (Fig. 1b, Supplementary Figs. S2, S3) with expression levels of TPCN1 usually being higher than those of TPCN2 (Fig. 1b, Supplementary Fig. S3). The size of the detected mRNA transcripts corresponds well to the size of the predicted sequence (4,705 bp for TPCN1 and 2,909 bp for TPCN2). Upon heterologous expression in HEK293 or COS-7 cells, both TPCN1 and TPCN2 are strictly localized in intracellular compartments (Figs. 1c, 2). Removal of the cytosolic N- and C-termini, as well as deletion of cryptic ER retention signals [33], present in the primary sequences of TPCN1 or TPCN2 (dileucine motifs starting at position 8 and 692 and a RxR motive starting at position 313 in TPCN2) did not result in increased expression in the

plasma membrane (not shown). Two protein bands were detected in immunoblots for either TPCN1 or TPCN2 (Fig. 1d, left lanes in left and middle panels, see also Supplementary Fig. S4 for generation and validation of the TPCN2 antibody). The respective lower bands represent the core-glycosylated proteins since they are shifted to slightly lower molecular weights after incubation with endoglycosidase H (EndoH). The upper band corresponds to the fully glycosylated mature channel which is resistant to Endo H and is sensitive to treatment with N-glycosidase F (PNGase F). Mutation of the two putative N-glycosylation sites in TPCN2 (N594 and N601) resulted in the production of a non-glycosylated protein (Fig. 1d, right panel). The size of the non-glycosylated TPCN1 and TPCN2 proteins was smaller than predicted from the primary sequence (78.5

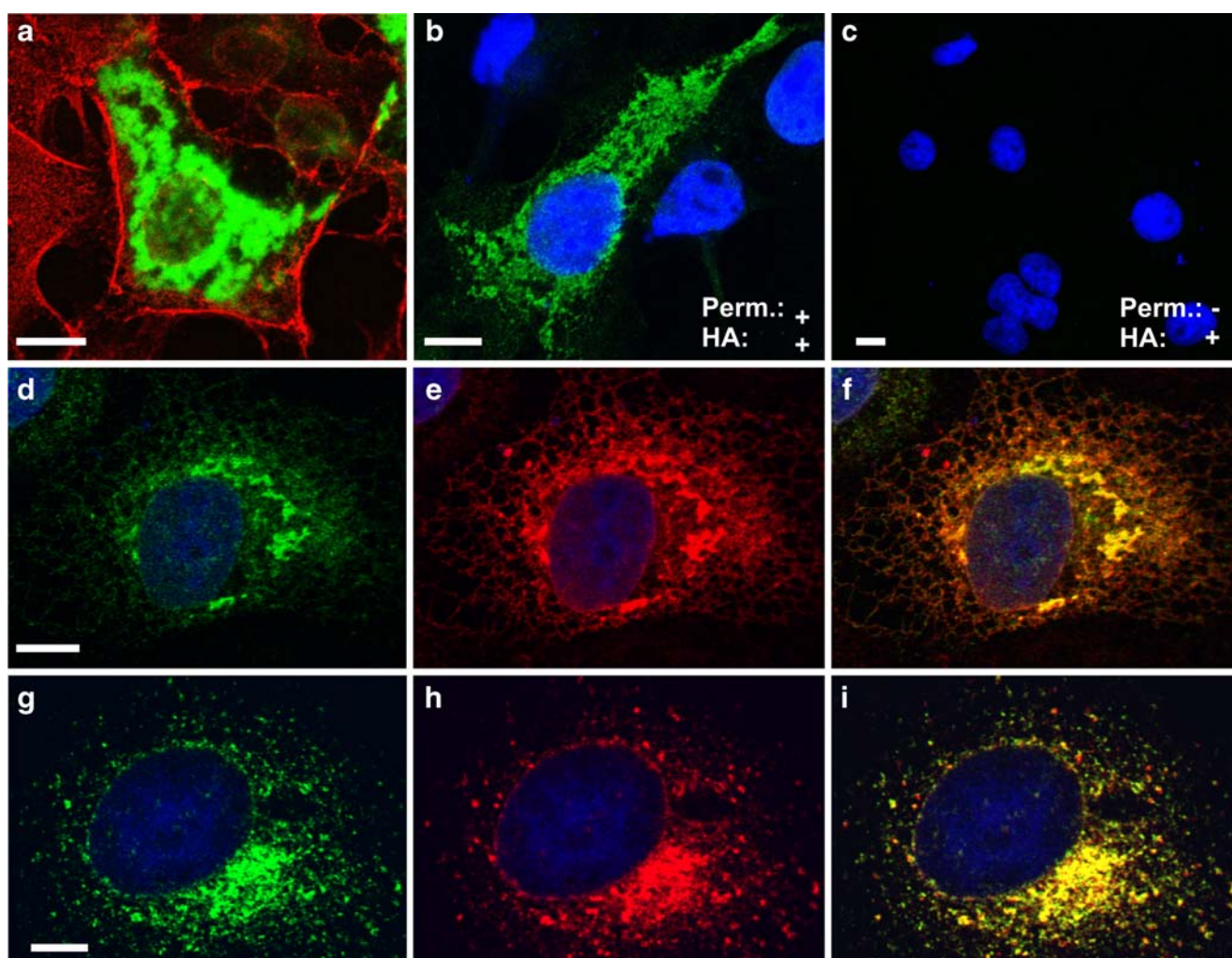


**Fig. 2** TPCN2 is localized in the lysosomes. Immunocytochemistry of TPCN2 in COS-7 cells. **a** Strong TPCN2 staining (green) is observed in intracellular compartments. By contrast, TPCN2 is absent from the plasma membrane (visualized in red by a specific marker). **b** After permeabilization, HA-tagged TPCN2 is detected intracellularly. **c** HA-tagged TPCN2 is not detected in the membrane of non

permeabilized cells. **d–f** Colocalization of TPCN2 (green) and the ER marker protein calnexin (red). Most TPCN2-positive structures (**d**) costain for endoplasmic reticulum (**e**), yielding yellow in the overlay (**f**). **g–i** Colocalization of TPCN2 (green) and lamp1 (red). Most TPCN2-positive structures (**g**) costained for lysosomes (**h**), yielding yellow in the overlay (**i**). (bars 10  $\mu\text{m}$ )

vs. 94.3 kDa for TPCN1 and 63 vs. 83.5 kDa for TPCN2). The apparent smaller molecular weight very likely arises from an aberrant gel mobility of the two proteins because it was also observed with EGFP-tagged TPCN channel proteins and with antibodies that were targeted to either N- or C-termini. Given the principal topology of pore-loop cation channels, it is very likely that two TPCN channel subunits assemble to form a complex with pseudo-tetrameric symmetry. Indeed, co-immunoprecipitation experiments showed that TPCN2 assembles with each other to form homomers (Fig. 1e). By contrast, TPCN2 did not form immunocomplexes with TPCN1 indicating that TPCN2–TPCN1 heteromers are not formed in the cell (Fig. 1e).

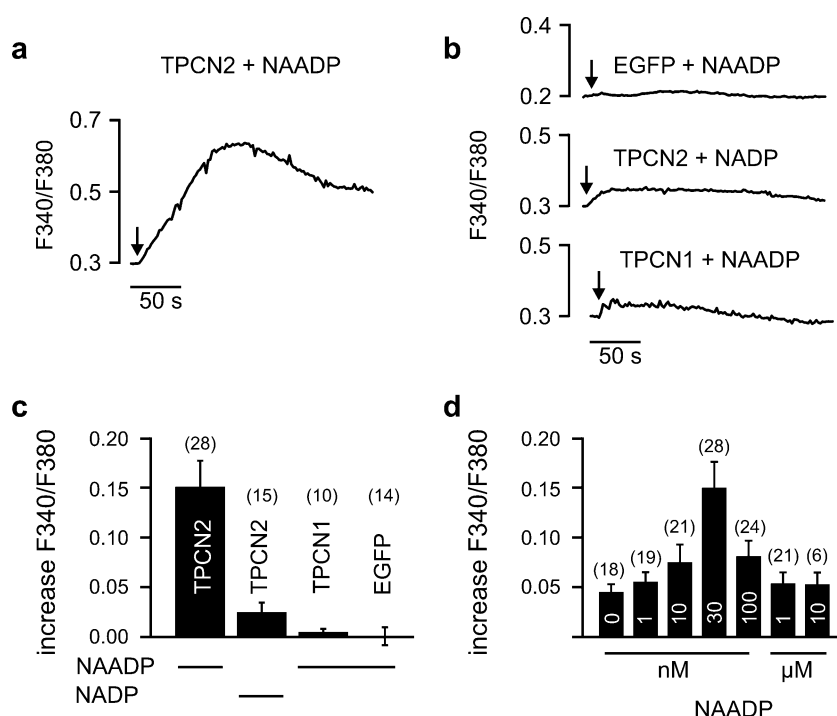
We next analyzed the subcellular expression of heterologously expressed TPCN2 in COS-7 cells. Using wild-type TPCN2 (Fig. 2a) and TPCN2 channels carrying a HA tag in the linker region between S1 and S2 (Fig. 2b, c), we confirmed that the channel is expressed purely in intracellular compartments. Within the cell, TPCN2 was present in the ER (Fig. 2d–f) and colocalized with the lysosomal-associated membrane protein 1 (lamp1) that is a specific marker for acidic lysosomes (Fig. 2g–i, Supplementary Fig. S5). By contrast, there was no significant overlap of the TPCN2 signal with a mitochondrial marker (MitoTracker, Supplementary Fig. S6).

The presence of TPCN2 in the ER and in lysosomes suggested that the protein may be a candidate for the NAADP-sensitive release channel [10, 13, 15]. In order to test this hypothesis, we measured calcium transients by using Fura-2 fluorescence in HEK293 cells (Fig. 3). Fluorescence

was measured in the whole-cell patch-clamp configuration with a  $\text{Ca}^{2+}$ -free extracellular solution to ensure that changes in fluorescence were due to intracellular release. Cells transfected with TPCN2 that was N-terminally fused with EGFP to monitor expression (Supplementary Fig. S4) showed a similar basal  $\text{Ca}^{2+}$  concentration ( $62.9 \pm 21.4$  nM;  $n=15$ ) as control cells transfected with EGFP alone ( $50.6 \pm 19.5$  nM;  $n=8$ ). Intracellular application of 30 nM NAADP produced a robust  $\text{Ca}^{2+}$  transient in TPCN2-transfected cells (Fig. 3a, c). The peak  $\text{Ca}^{2+}$  concentration was  $292 \pm 54.9$  nM ( $n=28$ ) which is in excellent agreement with  $\text{Ca}^{2+}$  concentrations obtained in native cells after stimulation by NAADP [24, 28]. By contrast, control cells transfected with EGFP did not respond to NAADP ( $P < 0.001$ ; Fig. 3b, upper trace). Moreover, a close structural homolog of NAADP, NADP [15] did not yield a  $\text{Ca}^{2+}$  transient in TPCN2-transfected cells ( $P < 0.001$ ; Fig. 3b, middle trace). Remarkably, cells transfected with a TPCN1-EGFP fusion protein displayed no NAADP-sensitive  $\text{Ca}^{2+}$ -release ( $P < 0.001$ ). The dose–response curve of TPCN2 for NAADP has the typical bell-shape described for the native mammalian release channel [8, 22] (Fig. 3d). The channel starts to get activated in the low nanomolar range of NAADP, reaches a peak at about 30 nM and inactivated at higher concentrations of NAADP. At micromolar NAADP concentrations, the channel is totally inactive.

In HEK293 and COS-7 cells, TPCN2 was localized in the ER and the lysosomes. We tested from which of these compartments the observed  $\text{Ca}^{2+}$ -release was originating. Preincubation of the cells with bafilomycin, a specific

**Fig. 3** NAADP triggers  $\text{Ca}^{2+}$ -release in HEK293 cells transfected with TPCN2. Application of 30 nM NAADP via the patch pipette induces  $\text{Ca}^{2+}$ -release from internal stores in cells transfected with TPCN2-EGFP (a) but not in cells transfected with EGFP alone (b, upper panel) or cells transfected with TPCN1-EGFP (b, lower panel). In cells transfected with TPCN2-EGFP, NADP (30 nM; negative control) did not induce  $\text{Ca}^{2+}$ -release (b, middle panel). The arrows in a, b indicate the start of cell perfusion. c Population data for experiments performed in (a, b). d Dose–response relationship of NAADP. All values are given as mean  $\pm$  SEM. Number of cells measured is indicated in brackets in (c) and (d)



blocker of the vacuolar type- $H^+$  ATPase [5], almost completely abolished NAADP-mediated  $Ca^{2+}$ -release (Fig. 4a, d). By contrast, when ER stores were depleted by preincubation with the  $Ca^{2+}$ -ATPase inhibitor thapsigargin, NAADP-sensitive  $Ca^{2+}$ -release was not significantly reduced (Fig. 4b, d).  $IP_3$  which opens  $IP_3$ Rs in the ER induced  $Ca^{2+}$ -release in control cells but did not evoke  $Ca^{2+}$  transients in thapsigargin-pretreated cells ( $P<0.001$ ), demonstrating that the ER is functionally intact in TPCN2 expressing cells (Fig. 4c, d). These findings indicate that the observed  $Ca^{2+}$ -release in TPCN2 expressing cells arises from lysosomal stores while the channel in the ER is functionally silent. The reason for the lack of activity of the channel in the ER has to be determined. However, one may speculate that TPCN2 requires an acidic pH as present in the lysosomes and/or the assembly with proteins specifically expressed in lysosomes to acquire biological activity.

## Discussion

Here, we show that TPCN2, a novel member of the two-pore cation channel family, displays the basic functional

properties of the native NAADP-dependent  $Ca^{2+}$ -release channel. TPCN2 transcripts are widely expressed in the body and have been found in all tissues and organs investigated. TPCN2 encodes a glycosylated 75 kD protein forming homomers. Given the principal transmembrane topology of pore-loop cation channels, it is very likely that two TPCN channel subunits assemble with each other to form a complex with pseudo-tetrameric symmetry. This finding is in principal agreement with the reported molecular mass of the NAADP receptor of approximately 120 kDa [2, 9] that roughly corresponds to a TPCN2 dimer. The TPCN2 protein is specifically localized in intracellular compartments and is totally absent from the plasma membrane. Within the cells, the protein was present in acidic lysosomes and in the ER. Since our functional studies strongly indicate that only the lysosomal fraction of TPCN2 is sensitive to NAADP, the presence of TPCN2 in the ER probably reflects an overexpression phenomenon, as reported for other proteins, including ion channels [27].

Several lines of evidence support the notion that TPCN2 is a key component of long-sought lysosomal NAADP receptor. First of all, TPCN2 is the first channel identified that responds to NAADP in the correct physiological

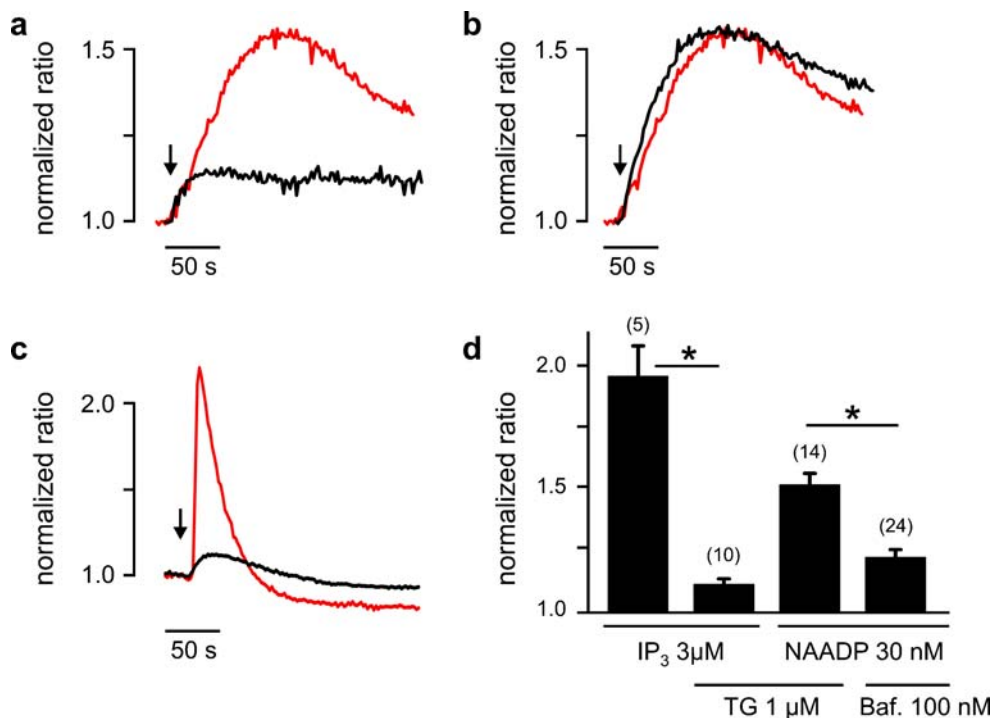


**Fig. 4** TPCN2 mediates NAADP-dependent  $Ca^{2+}$ -release from lysosomes. **a** In HEK293 cells transfected with TPCN2-EGFP, preincubation (45 min) with 100 nM bafilomycin almost completely abolished NAADP (30 nM)-induced  $Ca^{2+}$ -release (black line). Red line control without pretreatment. **b** In HEK293 cells transfected with TPCN2-EGFP, preincubation (15 min) with 1  $\mu$ M thapsigargin did not reduce NAADP-sensitive  $Ca^{2+}$ -release (black line). Red line same control as in (a). **c** Effect of thapsigargin (1  $\mu$ M) on the  $IP_3$  (3  $\mu$ M)-

induced  $Ca^{2+}$ -release. Experiments were performed either with (black line) or without (red line) thapsigargin preincubation (1  $\mu$ M; 15 min). Arrows in (a–c) indicate the start of cell perfusion. **d** Population data for experiments shown in (a–c). Number of cells measured is indicated in brackets. Tg thapsigargin; Baf bafilomycin;  $IP_3$  Inositol-1,4,5-trisphosphate. Fluorescent ratio were normalized for better comparison



concentration range (low nM) [14]. Secondly, as described for native channels, TPCN2 is inactivated by micromolar NAADP concentrations [8, 22]. Thirdly, the channel is insensitive to the NAADP homolog NADP [15]. Also, the homologous TPCN1 channel is totally insensitive to NAADP. Fourthly, the increase in the intracellular  $\text{Ca}^{2+}$  concentration in cells expressing TPCN2 was in the same range as described for native NAADP-release channels [24, 28]. Fifthly, TPCN2 is localized in the acidic lysosomes, the subcellular organelles where NAADP-dependent  $\text{Ca}^{2+}$ -release was originally described [10]. Importantly, TPCN2 activity is abolished by maneuvers that deplete the lysosomes [10, 13] indicating that the protein is fully operative in these organelles. By contrast, TPCN2 present in the ER was functionally silent. While we cannot exclude that TPCN2 requires assembly with another cellular protein to form a functional  $\text{Ca}^{2+}$ -release channel, the simplest interpretation of our work is that TPCN2 itself forms the lysosomal NAADP-sensitive  $\text{Ca}^{2+}$ -release channel. Further in vivo studies will be required to dissect the signaling cascades that control activation and modulation of TPCN2.

**Acknowledgements** Lamp1-EGFP was a kind gift of Esteban C. Dell'Angelica (Dept Human Genetics, UCLA; USA). This work was supported by the Deutsche Forschungsgemeinschaft (DFG).

**Open Access** This article is distributed under the terms of the Creative Commons Attribution Noncommercial License which permits any noncommercial use, distribution, and reproduction in any medium, provided the original author(s) and source are credited.

Note added in proof: during the submission process, a paper was published presenting similar findings that TPCN2 mediates NAADP-dependent  $\text{Ca}^{2+}$ -release from acidic organelles [7].

## References

1. Beck A, Kolisek M, Bagley LA, Fleig A, Penner R (2006) Nicotinic acid adenine dinucleotide phosphate and cyclic ADP-ribose regulate TRPM2 channels in T lymphocytes. *FASEB J* 20:962–964
2. Berridge G, Dickinson G, Parrington J, Galione A, Patel S (2002) Solubilization of receptors for the novel  $\text{Ca}^{2+}$ -mobilizing messenger, nicotinic acid adenine dinucleotide phosphate. *J Biol Chem* 277:43717–43723
3. Berridge MJ, Lipp P, Bootman MD (2000) The versatility and universality of calcium signalling. *Nat Rev Mol Cell Biol* 1:11–21
4. Boittin FX, Galione A, Evans AM (2002) Nicotinic acid adenine dinucleotide phosphate mediates  $\text{Ca}^{2+}$  signals and contraction in arterial smooth muscle via a two-pool mechanism. *Circ Res* 91:1168–1175
5. Bowman EJ, Siebers A, Altendorf K (1988) Bafilomycins: a class of inhibitors of membrane ATPases from microorganisms, animal cells, and plant cells. *Proc Natl Acad Sci U S A* 85:7972–7976
6. Broad LM, Armstrong DL, Putney JW Jr (1999) Role of the inositol 1,4,5-trisphosphate receptor in  $\text{Ca}^{2+}$  feedback inhibition of calcium release-activated calcium current (I<sub>crac</sub>). *J Biol Chem* 274:32881–32888
7. Calcraft PJ, Ruas M, Pan Z, Cheng X, Arredouani A, Hao X, Tang J, Rietdorf K, Teboul L, Chuang KT, Lin P, Xiao R, Wang C, Zhu Y, Lin Y, Wyatt CN, Parrington J, Ma J, Evans AM, Galione A, Zhu MX (2009) NAADP mobilizes calcium from acidic organelles through two-pore channels. *Nature* 459:596–600
8. Cancela JM, Churchill GC, Galione A (1999) Coordination of agonist-induced  $\text{Ca}^{2+}$ -signalling patterns by NAADP in pancreatic acinar cells. *Nature* 398:74–76
9. Churamani D, Dickinson GD, Patel S (2005) NAADP binding to its target protein in sea urchin eggs requires phospholipids. *Biochem J* 386:497–504
10. Churchill GC, Okada Y, Thomas JM, Genazzani AA, Patel S, Galione A (2002) NAADP mobilizes  $\text{Ca}^{2+}$  from reserve granules, lysosome-related organelles, in sea urchin eggs. *Cell* 111:703–708
11. Clapham DE (2007) Calcium signaling. *Cell* 131:1047–1058
12. Clapham DE, Garbers DL (2005) International Union of Pharmacology. L. Nomenclature and structure-function relationships of CatSper and two-pore channels. *Pharmacol Rev* 57:451–454
13. Galione A, Petersen OH (2005) The NAADP receptor: new receptors or new regulation? *Mol Interv* 5:73–79
14. Galione A, Ruas M (2005) NAADP receptors. *Cell Calcium* 38:273–280
15. Gerasimenko JV, Maruyama Y, Yano K, Dolman NJ, Tepikin AV, Petersen OH, Gerasimenko OV (2003) NAADP mobilizes  $\text{Ca}^{2+}$  from a thapsigargin-sensitive store in the nuclear envelope by activating ryanodine receptors. *J Cell Biol* 163:271–282
16. Grynkiewicz G, Poenie M, Tsien RY (1985) A new generation of  $\text{Ca}^{2+}$  indicators with greatly improved fluorescence properties. *J Biol Chem* 260:3440–3450
17. Guse AH, Lee HC (2008) NAADP: a universal  $\text{Ca}^{2+}$  trigger. *Sci Signal* 1:re10
18. Ishibashi K, Suzuki M, Imai M (2000) Molecular cloning of a novel form (two-repeat) protein related to voltage-gated sodium and calcium channels. *Biochem Biophys Res Commun* 270:370–376
19. Lee HC (2001) Physiological functions of cyclic ADP-ribose and NAADP as calcium messengers. *Annu Rev Pharmacol Toxicol* 41:317–345
20. Lee HC, Aarhus R (1995) A derivative of NADP mobilizes calcium stores insensitive to inositol trisphosphate and cyclic ADP-ribose. *J Biol Chem* 270:2152–2157
21. Malavasi F, Deaglio S, Funaro A, Ferrero E, Horenstein AL, Ortolan E, Vaisitti T, Aydin S (2008) Evolution and function of the ADP-ribosyl cyclase/CD38 gene family in physiology and pathology. *Physiol Rev* 88:841–886
22. Masgrau R, Churchill GC, Morgan AJ, Ashcroft SJ, Galione A (2003) NAADP: a new second messenger for glucose-induced  $\text{Ca}^{2+}$  responses in clonal pancreatic beta cells. *Curr Biol* 13:247–251
23. Mikoshiba K (2007) IP<sub>3</sub> receptor/ $\text{Ca}^{2+}$  channel: from discovery to new signaling concepts. *J Neurochem* 102:1426–1446
24. Morgan AJ, Galione A (2007) NAADP induces pH changes in the lumen of acidic  $\text{Ca}^{2+}$  stores. *Biochem J* 402:301–310
25. Much B, Wahl-Schott C, Zong X, Schneider A, Baumann L, Moosmang S, Ludwig A, Biel M (2003) Role of subunit heteromerization and N-linked glycosylation in the formation of functional hyperpolarization-activated cyclic nucleotide-gated channels. *J Biol Chem* 278:43781–43786
26. Peiter E, Maathuis FJ, Mills LN, Knight H, Pelloux J, Hetherington AM, Sanders D (2005) The vacuolar  $\text{Ca}^{2+}$ -activated channel TPC1 regulates germination and stomatal movement. *Nature* 434:404–408



27. Schroeder BC, Waldegger S, Fehr S, Bleich M, Warth R, Greger R, Jentsch TJ (2000) A constitutively open potassium channel formed by KCNQ1 and KCNE3. *Nature* 403:196–199
28. Steen M, Kirchberger T, Guse AH (2007) NAADP mobilizes calcium from the endoplasmic reticular Ca(2+) store in T-lymphocytes. *J Biol Chem* 282:18864–18871
29. Streb H, Irvine RF, Berridge MJ, Schulz I (1983) Release of Ca<sup>2+</sup> from a nonmitochondrial intracellular store in pancreatic acinar cells by inositol-1,4,5-trisphosphate. *Nature* 306:67–69
30. Wahl-Schott C, Baumann L, Cuny H, Eckert C, Griessmeier K, Biel M (2006) Switching off calcium-dependent inactivation in L-type calcium channels by an autoinhibitory domain. *Proc Natl Acad Sci U S A* 103:15657–15662
31. Yu FH, Catterall WA (2004) The VGL-kanome: a protein superfamily specialized for electrical signaling and ionic homeostasis. *Sci STKE* 2004:15
32. Zalk R, Lehnart SE, Marks AR (2007) Modulation of the ryanodine receptor and intracellular calcium. *Annu Rev Biochem* 76:367–385
33. Zerangue N, Schwappach B, Jan YN, Jan LY (1999) A new ER trafficking signal regulates the subunit stoichiometry of plasma membrane K(ATP) channels. *Neuron* 22:537–548
34. Zhang F, Jin S, Yi F, Li PL (2008) TRP-ML1 functions as a lysosomal NAADP-sensitive Ca(2+) release channel in coronary arterial myocytes. *J Cell Mol Med*. doi:[10.1111/j.1582-4934.2008.00486.x](https://doi.org/10.1111/j.1582-4934.2008.00486.x)